

Direct Determination of Hydrogen-Bonded Structures in Resonant and Tautomeric Reactions Using Ultrafast Electron Diffraction

Ramesh Srinivasan, Jonathan S. Feenstra, Sang Tae Park, Shoujun Xu, and Ahmed H. Zewail*

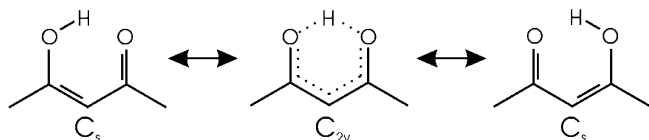
Laboratory for Molecular Sciences, Arthur Amos Noyes Laboratory of Chemical Physics, California Institute of Technology, Pasadena, California 91125

Received December 23, 2003; E-mail: zewail@caltech.edu

Hydrogen bonds are ubiquitous in chemistry and biology. While the strength of the “classical hydrogen bond” is around 3–5 kcal/mol, hydrogen-bond strengths span more than 2 orders of magnitude (0.2–40 kcal/mol), with the nature of the hydrogen bond (HB) varying as a function of its electrostatic, dispersion, charge-transfer, and covalent contributions.¹ In the extreme limit, for symmetric HBs X–H–X, the H-atom is equally shared; no distinction can then be made between the donor and acceptor, or the “covalent” X–H and “noncovalent” H···X bond.² Such unusually strong interactions can result either from charge-transfer-assisted HBs in polarizable systems or from so-called resonance-assisted HBs due to conjugation in neutral systems.^{3,4}

Enolones, the enol tautomers of β -diketones, contain two neutral donor and acceptor oxygen atoms connected by a system of conjugated double bonds (Scheme 1); the consequent synergistic

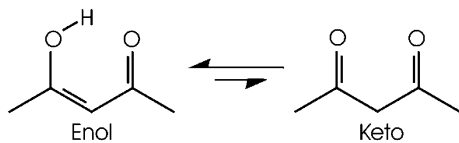
Scheme 1. Structures of Enolic Acetylacetone



reinforcement of H-bonding and π -delocalization can lead to strong intramolecular resonance-assisted O–H···O HBs. Increasing delocalization may transform the HB from an asymmetric O–H···O interaction (double well) to a symmetric O–H–O bond (single well), with the O···O distance being a measure of the strength of the HB. In the limit of complete delocalization, the C–C and C=C bonds as well as the C–O and C=O bonds become equal to each other, the O···O distance becomes very short, and the H-atom lies midway between the two oxygens. Acetylacetone (AcAc), a prototypical enolone, has been the subject of numerous experimental^{5–17} and theoretical^{18–24} efforts to understand the nature of such strong HBs.

AcAc comprises two tautomeric forms in dynamic equilibrium, with the enol form dominating in the gas phase at room temperature due to stabilization by the internal HB (Scheme 2).^{12,18} Previous

Scheme 2. Enol–Keto Tautomerization by Hydrogen Shift



gas-phase electron diffraction experiments present conflicting enol structures: Lowrey et al.⁵ and Andreassen and Bauer⁶ report a symmetric (C_{2v}) structure with a symmetric, linear HB, while Iijima et al.⁷ support an asymmetric (C_s) structure with an asymmetric, bent HB. Surprisingly, the two experiments reporting a symmetric

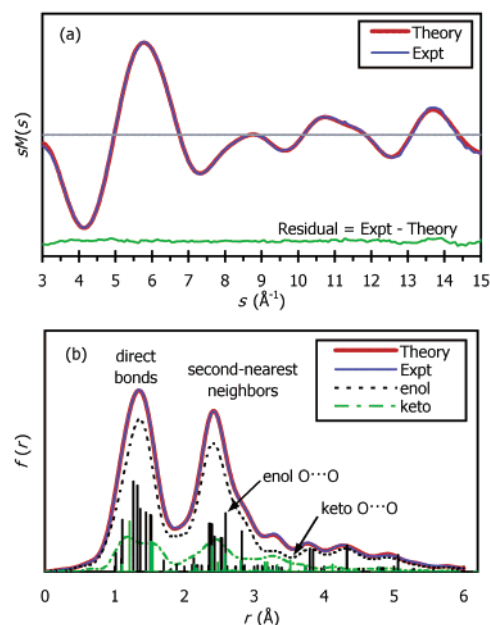


Figure 1. Diffraction data and structural refinement of acetylacetone. (a) Modified molecular scattering intensity, $sM(s)$. (b) Total and species radial distribution curves, $f(r)$.

structure give very different O···O distances, (2.381 Å⁵ vs 2.514 Å⁶). Moreover, theoretical investigations remain unsettled on the relative energies of these structures,²⁰ placing C_{2v} anywhere from slightly below¹⁸ to >20 kcal/mol above²² the C_s structure.

In this communication we elucidate the keto–enol tautomeric equilibrium, the structure of both keto and enol forms, and the nature of the intramolecular O–H···O HB in enolic AcAc using electron diffraction—thereby resolving this long-standing controversy in the literature. With its proven ability to study complex molecular systems in thermal equilibrium,^{25–28} our third-generation ultrafast electron diffraction apparatus (UED-3)²⁸ was employed to study the gas-phase diffraction of ground-state AcAc (2,4-pentanedione, 99+%, Aldrich) at 155 °C.

Figure 1 shows the ground-state diffraction data: the modified molecular scattering intensity, $sM(s)$, and its sine Fourier transform, the radial distribution curve $f(r)$, whose peaks reflect the relative density of internuclear distances in the molecule.²⁵ The first peak at ~ 1.5 Å corresponds to direct bond distances in both the enol and keto forms, the peak at ~ 2.5 Å to second-nearest neighbor distances and the peaks at longer distances to the unique O···O and C···O distances in the enol and keto tautomers.

Structural determination of AcAc tautomers requires an accurate estimate of the relative populations of the enol and keto forms. Diffraction data were fit using a mixture of enol (C_s) and keto AcAc, with their starting geometries derived from density functional theory

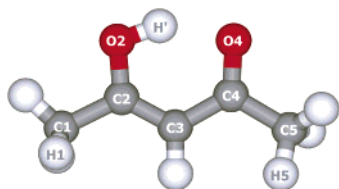


Figure 2. Final refined structure of the enol tautomer of acetylacetone. $r(\text{C1}-\text{C2}) = 1.504 \pm 0.021$, $r(\text{C2}-\text{C3}) = 1.359 \pm 0.034$, $r(\text{C3}-\text{C4}) = 1.443 \pm 0.019$, $r(\text{C4}-\text{C5}) = 1.518 \pm 0.023$, $r(\text{C2}-\text{O2}) = 1.321 \pm 0.021$, $r(\text{C4}-\text{O4}) = 1.262 \pm 0.005$, $\angle\text{C1}-\text{C2}-\text{C3} = 123.6 \pm 1.1$, $\angle\text{C2}-\text{C3}-\text{C4} = 120.4 \pm 1.0$, $\angle\text{C3}-\text{C4}-\text{C5} = 118.2 \pm 1.0$, $\angle\text{C1}-\text{C2}-\text{O2} = 112.9 \pm 2.7$, $\angle\text{C5}-\text{C4}-\text{O4} = 118.7 \pm 3.1$, $\angle\text{H1C1}-\text{C2C3} = -57.2 \pm 16.5$, $\angle\text{H5C5}-\text{C4C3} = -19.3 \pm 4.8$. Distances (r_c) are in Å, and angles are in degrees.

(DFT) calculations. Initial fitting of the populations of these DFT structures yielded an enol–keto ratio of $88:12 \pm 1$, which is in stark contrast to that expected at 155°C —thermodynamic equilibrium constants obtained by a variety of techniques (NMR, UV, IR)^{11–15} predict a ratio between 71:29 and 79:21 in the gas phase. To resolve this discrepancy, we revisited the starting geometry of the keto form which is free to undergo internal rotation about its C–C single bonds.^{18,19} The resultant array of keto rotamers was accounted for by floating the skeletal (and methyl) torsion angles of the DFT keto structure. The partially refined keto structure is quite different from that reported in the literature—the oxygen atoms are much further apart (~ 3.520 Å; dihedral $\angle\text{OCCO} = 104.7^\circ$) compared to that previously reported (~ 2.767 Å; dihedral $\angle\text{OCCO} = 48.6^\circ$).⁵

Refitting the equilibrium population using this partially refined keto structure gave $78:22 \pm 4$, in excellent agreement with the results of gas-phase NMR¹² and IR absorption,¹⁵ thus highlighting the crucial importance of keto internal rotation. It is pertinent to note here that simple calculations of equilibrium populations from DFT energies (using a fixed keto conformation) predict a ratio of $\sim 98:2$ at 155°C due to a serious underestimation of the entropic term (2.4 cal/mol/K); using the experimental^{12–14} value of 8.3 cal/mol/K, we in fact obtain a ratio of $\sim 80:20$. Furthermore, using a C_{2v} enolic model underestimates the ratio at $68:32 \pm 3$.

Structural refinement of the enol was then performed using the fit values for the equilibrium ratio and the keto geometry. Figure 1 shows the remarkable agreement between experiment and theory. The refined enolic structure is asymmetric, with all direct bond distances and angles being within ~ 0.02 Å and $\sim 3^\circ$ of the DFT values, respectively (Figure 2). Differences between the carbon–carbon distances (0.084 Å) and carbon–oxygen distances (0.059 Å) are far greater than the corresponding standard deviations and clearly distinguish between single and double bonds—a manifestation of structural asymmetry. The $\text{O}\cdots\text{O}$ distance of ~ 2.592 Å in this structure is longer than those previously reported by electron diffraction at room temperature (2.512 Å⁷) and X-ray crystallography (2.535^9 and 2.547 Å¹⁰). These studies, along with neutron scattering in crystals,⁸ liquid-phase NMR,¹⁷ and gas-phase vibrational spectroscopy,¹⁶ are consistent with an asymmetric structure. Due to the relatively weak scattering of the hydrogen atom, in our fit, the O–H and $\text{H}\cdots\text{O}$ distances and the O–H \cdots O angle were held at DFT values (1.003 Å, 1.683 Å, and 148.4° , respectively). In light of the insensitivity of electron diffraction to hydrogen, it is surprising that Iijima et al.⁷ report a significantly out-of-plane H-atom ($\angle\text{HOCC} = 26^\circ$) which, though in reasonable agreement with a then-available crystal structure,⁹ manifests as unusually large error bars (0.016 Å) in their fit O–H distance. A more recent X-ray crystal structure¹⁰ supports the H-atom to be nearly in the molecular plane; $\angle\text{HOCC} \approx 4^\circ$.

The diffraction results reported here shed new light on the nature of the hydrogen bond in resonant and tautomeric structures. The keto structure with its large internal rotation exhibits a rotation-averaged dihedral angle of $\sim 105^\circ$ between the carbonyls at the reported temperature. The enolic structure clearly indicates that AcAc does exhibit some π -delocalization, leading to shorter C–C, C–O and longer C=C, C=O bonds compared to “unperturbed” distances in enols.⁴ However, this delocalization is not strong enough to give a symmetric skeletal geometry. The resulting long $\text{O}\cdots\text{O}$ distance is significant in making the homonuclear O–H \cdots O hydrogen bond localized and asymmetric.

The dynamics of hydrogen motion (O–H \cdots O) involves not only the $\text{O}\cdots\text{O}$ coordinate but also changes in skeletal geometry. In a symmetric double-well picture with “left” and “right” structures, there are two (\pm) states (symmetric and antisymmetric), and the probability of finding the structure in either is 50%, independent of the interaction. The time scale for hydrogen motion depends on the total internal energy and the height of the barrier, which in turn depends on the $\text{O}\cdots\text{O}$ separation—for short enough values, the structure becomes that of a single well. On the ultrashort time scale, the potential is asymmetric.^{21,29} It would be interesting to resolve the dynamics in real time using the new developments of UED^{25,28} on this and higher-energy structures.

Acknowledgment. We thank Professor John D. Roberts and the three reviewers for helpful comments.

References

- Steiner, T. *Angew. Chem., Int. Ed.* **2002**, *41*, 48–76.
- Perrin, C. L.; Nielson, J. B. *Annu. Rev. Phys. Chem.* **1997**, *48*, 511–544.
- Strictly speaking, resonance involves the superposition of two or more structures with different electronic distributions but *identical* nuclear positions. Here, besides single- and double-bond electronic conjugation, motion of the hydrogen atom is also involved.
- (a) Gilli, G.; Bellucci, F.; Ferretti, V.; Bertolasi, V. *J. Am. Chem. Soc.* **1989**, *111*, 1023–1028. (b) Gilli, P.; Bertolasi, V.; Ferretti, V.; Gilli, G. *J. Am. Chem. Soc.* **1994**, *116*, 909–915.
- Lowrey, A. H.; George, C.; D’Antonio, P.; Karle, J. *J. Am. Chem. Soc.* **1971**, *93*, 6399–6403.
- Andreassen, A. L.; Bauer, S. H. *J. Mol. Struct.* **1972**, *12*, 381–403.
- Iijima, K.; Ohnogi, A.; Shibata, S. *J. Mol. Struct.* **1987**, *156*, 111–118.
- Johnson, M. R.; Jones, N. H.; Geis, A.; Horsewill, A. J.; Trommsdorff, H. P. *J. Chem. Phys.* **2002**, *116*, 5694–5700.
- Camerman, A.; Mastropaolo, D.; Camerman, N. *J. Am. Chem. Soc.* **1983**, *105*, 1584–1586.
- Boese, R.; Antipin, M. Y.; Bläser, D.; Lyssenko, K. A. *J. Phys. Chem. B* **1998**, *102*, 8654–8660.
- Harris, R. K.; Rao, R. C. *Org. Magn. Reson.* **1983**, *21*, 580–586.
- Folkendt, M. M.; Weiss-Lopez, B. E.; Chauvel, J. P., Jr.; True, N. S. *J. Phys. Chem.* **1985**, *89*, 3347–3352.
- Nakanishi, H.; Morita, H.; Nagakura, S. *Bull. Chem. Soc. Jpn.* **1977**, *50*, 2255–2261.
- Hush, N. S.; Livett, M. K.; Peel, J. B.; Willett, G. D. *Aust. J. Chem.* **1987**, *40*, 599–609.
- Powling, J.; Bernstein, H. J. *J. Am. Chem. Soc.* **1951**, *73*, 4353–4356.
- Tayyari, S. F.; Zeegers-Huyskens, Th.; Wood, J. L. *Spectrochim. Acta* **1979**, *35A*, 1289–1295.
- Egan, W.; Gunnarsson, G.; Bull, T. E.; Forsén, S. *J. Am. Chem. Soc.* **1977**, *99*, 4568–4572.
- Dannenbergh, J. J.; Rios, R. *J. Phys. Chem.* **1994**, *98*, 6714–6718.
- Ishida, T.; Hirata, F.; Kato, S. *J. Chem. Phys.* **1999**, *110*, 3938–3945.
- Bauer, S. H.; Wilcox, C. F. *J. Chem. Phys. Lett.* **1997**, *279*, 122–128.
- Sharafeddin, O. A.; Hinsen, K.; Carrington, T., Jr.; Roux, B. *J. Comput. Chem.* **1997**, *18*, 1760–1772.
- Mavri, J.; Grdadolnik, J. *J. Phys. Chem. A* **2001**, *105*, 2039–2044.
- Grabowski, S. J. *J. Phys. Org. Chem.* **2003**, *16*, 797–802.
- Delchev, V. B.; Mikosch, H.; St. Nikolov, G. *Monatsh. Chem.* **2001**, *132*, 339–348.
- Srinivasan, R.; Lobastov, V. A.; Ruan, C.-Y.; Zewail, A. H. *Helv. Chim. Acta* **2003**, *86*, 1763–1838.
- Goodson, B. M.; Ruan, C.-Y.; Lobastov, V. A.; Srinivasan, R.; Zewail, A. H. *J. Phys. Chem. Lett.* **2003**, *374*, 417–424.
- Ihee, H.; Goodson, B. M.; Srinivasan, R.; Lobastov, V. A.; Zewail, A. H. *J. Phys. Chem. A* **2002**, *106*, 4087–4103.
- Ihee, H.; Lobastov, V. A.; Gomez, U. M.; Goodson, B. M.; Srinivasan, R.; Ruan, C.-Y.; Zewail, A. H. *Science* **2001**, *291*, 458–462.
- Ando, K.; Hynes, J. T. *J. Phys. Chem. B* **1997**, *101*, 10464–10478.

JA031927C